

3 Methods

3.1 Molecular Biology

3.1.1 Polymerase chain reaction (PCR)

The polymerase chain reaction [64] was used for the amplification of double stranded DNA from a template with the help of a pair of 20-30 bp long oligonucleotides (primers), that are complementary to the 5' and 3' end, respectively, of the amplified sequence. In a repetitive cycle of melting of DNA, annealing of primers and strand synthesis with a thermostable DNA polymerase, a template fragment flanked by the primer sequences is produced in large quantities. Gene-specific PCR primers were designed to add recognition sites for restriction nucleases to the 5' and 3' end of the amplified DNA sequence (see 2.5.1). To allow directional cloning, recognition sites for different restriction nucleases were added with either primer. Vector-specific primers used for colony PCRs and sequencing are listed in 2.5.2.

To obtain inserts for cloning of genes into expression vectors, the cDNA sequences were amplified with *Pfu* polymerase that possesses proofreading activity (Table 3.1). Colony PCRs were used to identify positives clones after ligation. With a pipette tip, cells from a single colony were transferred into the PCR tube with *Taq* polymerase reaction mix (Table 3.2). PCR reactions with the *Tpc5* gene always had to be carried out according to the *Taq* protocol.

Compound	Final concentration
H ₂ O	to 80 µl
10x <i>Pfu</i> reaction buffer	1x
5' primer	0.5 µM
3' primer	0.5 µM
template DNA	0.1-0.3 ng/µl
DMSO	1.25 %
dNTPs	400 µM
<i>Pfu</i> polymerase	5 U

Table 3.1: Standard PCR with *Pfu* polymerase.

Compound	Final concentration
H ₂ O	to 20 µl
10x <i>Taq</i> reaction buffer	1x
5' primer	0.5 µM
3' primer	0.5 µM
betaine	1 M
DMSO	5 %
dNTPs	250 µM
<i>Taq</i> polymerase	0.5 U

Table 3.2: Standard colony PCR with *Taq* polymerase.

The standard PCR program used is given in Table 3.3. As an exception, PCRs with vector-specific primers for pQLink (pQTEV3U/pQTEV3L) on constructs containing multiple expression cassettes (see 3.1.7) were done with 59 °C annealing temperature and 5 min extension.

Segment	Step	Temperature [°C]	Duration [min:sec]
1	melting	94	2:00
2	melting	95	0:30
	annealing	56	1:00
	extension	72	2:00
cycles		25	
3	final extension	72	10:00
	hold	4	forever

Table 3.3: Standard PCR program.

3.1.2 Restriction digest

Double-stranded DNA (vector or PCR product) was cut with restriction endonucleases type II, that specifically recognize 4-8 bp long palindromic sequences [65]. Thus, sticky or blunt ends are created, that later can be ligated with cohesive ends. Purified PCR products or DNA from plasmid preparations were incubated with restriction enzymes according to manufacturers' instructions in the recommended buffers. Double digests were used that allow directional cloning. A standard reaction is given in Table 3.4. The reaction was incubated 8 h or overnight at 37 °C.

Compound	Amount
H ₂ O	to 60 µl
purified PCR reaction or plasmid preparation	50 µl 2-3 µg
restriction enzyme I	1 µl, 10-20 U
restriction enzyme II	1 µl, 10-20 U
100x BSA	0.6 µl
10x reaction buffer	6 µl

Table 3.4: Standard restriction digest reaction.

3.1.3 DNA purification

PCR reactions and DNA fragments obtained after restriction digest were purified using QIAquick spin columns (Qiagen) according to manufacturer's instructions. Empty vectors or PCR products were purified following the PCR purification protocol. If a plasmid already containing an insert was digested, the reaction was loaded on an agarose gel and the desired

fragment, vector or insert, was excised with a scalpel and further processed according to the gel extraction protocol.

3.1.4 Gel electrophoresis of DNA fragments

For separation, size determination and the estimation of concentration of DNA fragments, samples were loaded on a gel with 1% agarose in TAE buffer supplemented with $0.5 \mu\text{g ml}^{-1}$ ethidium bromide together with a DNA ladder that has known band sizes and concentrations. Electrophoresis was performed at constant current (220 mA) in TAE buffer. Gels were analyzed using a UV lamp and size and concentration of samples was estimated by comparison with the standard.

3.1.5 Ligation

The ligase from bacteriophage T4 catalyzes the formation of a phosphodiester bond between 5'-phosphate groups and neighboring 3'-hydroxyl groups of DNA [66]. This mechanism is used to ligate restriction-digested PCR fragments/inserts and vectors with cohesive ends. Inserts (500 bp average size) and vectors (4000 bp average size) were mixed in a molar ratio of ~ 2:1 as described in Table 3.5. Reactions were incubated at room temperature for 1-2 h and then transformed into competent *E. coli* DH5 α cells.

Compound	Amount
H ₂ O	to 15 μl
insert (~500 bp)	4 ng
vector (~4000bp)	10 ng
T4 ligase	1 U
10x reaction buffer	1.5 μl

Table 3.5: Standard ligation reaction.

3.1.6 Transformation of chemically competent *E. coli* cells

Chemically competent cells were produced according to the protocol by Hanahan [67]. A 1 ml LB over-night culture was diluted 1:100 in the same medium and grown at 37 °C to an OD₆₀₀ of 0.6. Cells were cooled down on ice and harvested at 4 °C by centrifugation for 5 min with 2500x g. The subsequent steps were carried out at 4 °C with prechilled buffer. The pellet was resuspended in 30 ml TFB1 buffer, incubated for 45 min and centrifuged as before. Cells were then resuspended in 8 ml TFB2 buffer, and 50 μl aliquots were flash-frozen in liquid nitrogen and stored at -70 °C.

For transformation, competent cells were thawed on ice before DNA was carefully added. Reactions were incubated on ice for 30 min, followed by a heat shock at 42 °C for 45 sec. 800 µl LB medium were added, the cells were shaken for 50 min at 37 °C and then streaked on LB plates containing appropriate antibiotics.

3.1.7 Ligation independent cloning (LIC)

To generate co-expression cassettes with the pQLink system [68], the cDNA sequences of interest were first cloned into pQLinkH using the *Bam*HI/*Not*I sites of the multiple cloning site. To combine two pQLinkH plasmids, one plasmid was digested with *Pac*I while the other was cleaved with *Swa*I (Table 3.6).

Compound	<i>Pac</i> I digests	<i>Swa</i> I digests
H ₂ O	to 10 µl	to 10 µl
10x reaction buffer	1 µl NEB 1	1 µl NEB 3
100x BSA	0.1 µl	0.1 µl
plasmid	0.5 µg	0.5 µg
enzyme	0.5 µl <i>Pac</i> I, 5U	0.5 µl <i>Swa</i> I, 5U

Table 3.6: Protocol for *Pac*I and *Swa*I restriction digest.

Reactions were incubated over night at 37 °C (*Pac*I) or 25 °C (*Swa*I) and then heat-inactivated at 65 °C for 20 min. Samples were treated with T4 polymerase in the presence of dCTP (*Pac*I) or dGTP (*Swa*I).

Compound	<i>Pac</i> I reaction	<i>Swa</i> I reaction
H ₂ O	to 20 µl	to 20 µl
10x T4 buffer	2 µl	2 µl
100x BSA	0.1 µl	0.1 µl
digested sample	3 µl	3 µl
T4 polymerase	0.5 µl, 1.3U	0.5 µl, 1.3U
nucleotide	2.5 mM dCTP	2.5 mM dGTP

Table 3.7: T4 polymerase treatment of *Pac*I or *Swa*I digested plasmids.

Upon incubation for 30 min at 25 °C and heat inactivation at 65 °C for 20 min, 3 µl of each reaction were mixed and, to achieve annealing, heated to 65 °C for 1 min and cooled to room temperature. 2 µl 25 mM EDTA was added and the complete reaction was subjected to *E. coli* transformation.

3.1.8 Transformation of *S. cerevisiae*

A pre-culture of yeast cells was diluted to obtain a 30 ml culture with an OD₆₀₀ of 0.3. Cells were grown to an OD₆₀₀ of 0.8-1.0 and centrifuged at 500x g for 5 min, washed with 10 ml water and centrifuged again. The pellet was resuspended in 1 ml 0.1 M Lithium acetate, 1 M sorbitol. Cells were shaken for 30 min at 30 °C and directly used for transformation (Table 3.8).

Compound	Amount
yeast cells	40 µl
PEG mix	230 µl
ssDNA (10 mg ml ⁻¹)	5 µl
plasmid	5 µl

Table 3.8: Transformation reaction of yeast cells.

Reactions were incubated at 30 °C for 30 min, 30 µl DMSO were added followed by a heat shock at 42 °C for 7 min. Samples were then plated on selective SD plates.

3.1.9 Plasmid preparations

Clones on ligation plates were checked with colony PCR to identify plasmids containing the desired insert. Positive colonies were used to inoculate LB culture for mini (2 ml) or maxi (150 ml) plasmid preparations. The plasmid isolation was performed using the QIAprep Spin Miniprep Kit and QIAGEN Plasmid Maxiprep Kit according to manufacturer's instructions (Qiagen).

3.1.10 QuikChange mutagenesis (QCM)

Mutations were introduced using site-directed mutagenesis following a 2-stage protocol described by Wang and Malcolm [69]. Pairs of complementary 40-50 bp synthetic oligonucleotides were used that differ from the template sequence at the mutation sites. Base changes were in the middle of the oligos (see 2.5.3).

In the first step of mutagenesis, 5 PCR cycles with the 5' and 3' primers in separate tubes (Table 3.9) were performed before reactions were mixed and more PCR cycles were carried out. The standard program used for QuikChange mutagenesis is listed in Table 3.10.

Compound	Forward reaction	Reverse reaction
H ₂ O	to 50 µl	to 50 µl
10x <i>Pfu</i> reaction buffer	5 µl	5 µl
5' primer	0.5 µM	-
3' primer	-	0.5 µM
plasmid DNA	40-100 ng	40-100 ng
dNTPs	400 µM	400 µM
Turbo <i>Pfu</i> polymerase	2.5 U	2.5 U

Table 3.9: Standard QCM reaction.

Segment	Step	Temperature [°C]	Duration [min:sec]
1	melting	95	0:30
2	melting	95	0:30
	annealing	55	0:30
	extension	68	10:00
cycles		5	
mix forward and reverse reaction			
3	melting	95	0:30
	annealing	55	0:30
	extension	68	10:00
cycles		20	
4	final extension	68	15:00
	hold	4	forever

Table 3.10: Standard program for QCM.

After amplification DNA was incubated with *DpnI* restriction nuclease for 8 h at 37 °C. During incubation the methylated template DNA from *E. coli* is destroyed whereas the synthetic DNA from PCR remains intact. The samples were subsequently transformed into chemically competent *E. coli* DH5α cells, plasmids were isolated and mutants were identified by sequencing.

3.1.11 RNA isolation

For isolation of total mRNA, 20-50 mg of a mouse organ were preserved in 0.5 ml RNAlater RNA stabilization reagent (Qiagen) immediately after sacrificing the animal. The tissue was disrupted using an ultratorax tissue homogenizer and samples were subsequently processed with the RNeasy Mini Kit (Qiagen) according to manufacturer's instructions. Concentration of RNA was determined by measuring the OD₂₆₀ using an extinction coefficient $\epsilon_{260}=0.025 \text{ ml } (\mu\text{g cm})^{-1}$.

3.1.12 Quantitative real-time (RT) PCR

Total mRNA was transcribed to cDNA with M-MLV reverse transcriptase (H-) (Promega) and oligo-dT₁₅ primer (Table 3.11). RNA and oligo-dT₁₅ were preincubated at 70 °C for 5 min and cooled on ice for 5 min before the remaining compounds were added.

Compound	Amount
total RNA	1 μg
oligo-dT ₁₅	1 μg
5x reaction buffer	5 μl
dNTPs	250 μM
MLV RT (H-)	200 U
H ₂ O	to 50 μl

Table 3.11: Standard reverse transcriptase reaction.

Reactions were incubated for 10 min at 40 °C and then for 50 min at 42 °C.

RT-PCR was performed in triplicates with the QuantiTect SYBR Green PCR Kit (Qiagen) according to manufacturer's instructions with iCycler (Bio-Rad) using specific primers for the *bet3*, *tpc6a* and *tpc6b* coding sequences (see 2.5.4). One PCR product of expected size was obtained with each primer pair and sequenced, confirming amplification of the correct variant. After each PCR cycle, amplification curves were measured with the fluorescence from binding of the dye to the DNA. For quantification, a vector dilution from 2×10^8 to 2×10^3 copy numbers per reaction of pGEM-*bet3*, pGEM-*tpc6a* or pGEM-*tpc6b* was used to correlate amplification curves with copy numbers with the standard curve method. Measurements were carried out in triplicates and data were normalized with GAPDH expression levels.

Compound	Amount
cDNA	2 μ l
2x QuantiTect SYBR Green PCR mix	10 μ l
5' primer	0.3 μ M
3' primer	0.3 μ M
External well factor solution (100x)	0.2 μ l
H ₂ O	to 20 μ l

Table 3.12: Standard RT-PCR reaction.

Segment	Step	Temperature [°C]	Duration [min:sec]
1	activation	95	15:00
2	denaturation	94	0:15
	annealing	56	0:30
	extension	72	0:30
cycles		35	

Table 3.13: Standard RT-PCR program.

3.2 Protein purification and characterization

3.2.1 Expression in *Escherichia coli*

The expression constructs were transformed into *E. coli* SCS1 Rosetta or *E. coli* BL21 (DE3) cells. An overnight culture was inoculated in SB medium or LB medium containing appropriate antibiotics (100 $\mu\text{g ml}^{-1}$ ampicillin; 34 $\mu\text{g ml}^{-1}$ chloramphenicol; 30 $\mu\text{g ml}^{-1}$ kanamycin). The pre-culture was diluted 20-fold in the same medium and grown at 37 °C to an OD₆₀₀ of ~1.5 (SB medium) or OD₆₀₀ of ~0.7 (LB medium). After induction with 1 mM isopropyl-1-thio- β -D-galactopyranoside (IPTG), growth was continued for 4 h. For expression at 20 °C, cells were grown to an OD₆₀₀ of ~0.6 at 37 °C and cooled down to 20 °C prior to induction with 1 mM IPTG. Growth was continued at 20 °C over night. Cells were harvested by centrifugation at 5000x *g* for 10 min and pellets were stored at -20 °C.

3.2.2 Expression in *Saccharomyces cerevisiae*

Plasmids for expression in yeast were transformed into the *S. cerevisiae* strain AH22*ura3* (MATa, *ura3* Δ , *leu2-23,112*, *his4-519*, *can1*) and transformants were selected on SD -ura plates. For expression under the control of the inducible *CUP1* promoter of the yeast metallothionein gene, cells were grown 28 °C in WMVIII minimal medium with 40 mg ml⁻¹ histidine to an OD₆₀₀ of 1 and induced with 1 mM CuSO₄ over night. Cells were harvested by centrifugation at 5000x *g* for 10 min and pellets were stored at -20 °C.

3.2.3 Production of seleno-methionine labeled protein

For production of seleno-methionine (SeMet)-labeled Tpc6B, the pQTEV-*Tpc6B* plasmid was transformed into *E. coli* B834 (DE3), and cells were grown essentially as described by Budisa *et al.* [70]. A pre-culture in LB medium was grown for one day and cells were harvested and washed with new minimal medium (NMM). The culture was diluted 1:100 with NMM containing 20% methionine and 80% SeMet (25 $\mu\text{g ml}^{-1}$ total concentration) and grown over night. Cells were again washed with NMM and diluted 1:100 in NMM containing 100% SeMet. The culture was induced with 1 mM IPTG when an OD₆₀₀ of 0.4-0.8 was reached (approximately 24 h later).

3.2.4 Cell lysis

During lysis cells were constantly cooled on ice to avoid heating of the samples. The cell pellets were resuspended in the appropriate buffer supplemented with additives (see 3.2.5).

Lysis by sonication was performed with a SH213G sonicator (Bandelin electronics) set to 90% power twice for 10 sec. Alternatively, cells were opened by passing the suspension twice through a French Press (SLM-AMINCO) at 1100 psi (7.6 MPa) pressure. A cleared lysate was obtained by centrifugation at 40,000x g for 30 min.

3.2.5 Affinity chromatography

The initial step of each purification protocol would be an affinity chromatography carried out as batch purification. Cells from a 2 l culture (~5 g pellet) were lysed in 35 ml buffer and applied to 2 ml of affinity matrix. After incubation for 1-2 h, the suspension was transferred into a polypropylene column. Washing and elution steps were done with gravity flow through the self-poured column.

3.2.5.1 Purification with Ni-nitrilotriacetate (NTA) agarose

Fusion proteins carrying an oligo-histidine tag (6x His-tag or 7x His-tag) can be purified with Ni-nitrilotriacetate (Ni-NTA) matrix. NTA is coupled to sepharose CL-6B and chelates Ni²⁺ ions. The remaining ligand binding sites of Ni(II) can form a complex with histidine residues and thus binds His-tags. Elution is achieved by the addition of the histidine analog imidazole that will occupy the binding sites for histidine if present in excess.

Cells expressing His-tagged fusion protein were lysed in His-lysis buffer supplemented with 1 mM PMSF, one protease tablet Complete Mini EDTA-free, 3 mM β -mercaptoethanol and DNase I or Benzonase. After batch binding, the affinity matrix was washed extensively with His-wash buffer and eluted with His-elution buffer.

3.2.5.2 Purification with glutathione (GSH) sepharose

Glutathione (GSH) sepharose is used to bind proteins fused with a glutathion-S-transferase domain (GST-tag). The GST protein (~25 kDa) interacts specifically and with high affinity with its substrate GSH which is coupled to sepharose 4B. Elution of bound protein is achieved by the addition of soluble GSH that displaces the affinity matrix from GST.

Cells expressing GST-tagged fusion protein were lysed in PBS buffer supplemented with 1 mM PMSF, half a protease tablet Complete, 1 mM DTT and DNase I. After batch binding, the affinity matrix was washed extensively with PBS and eluted with GST-elution buffer.

3.2.5.3 Purification with Talon resin

Fusion proteins carrying a His-tag can be purified with Talon resin alternatively to Ni-NTA matrix. Talon resin works analogously to Ni-NTA but has Co^{2+} ions chelated resulting in a better specificity for oligo-histidine tags.

Yeast cells expressing His-tagged fusion protein were lysed in Yeast-lysis buffer supplemented with 1 mM PMSF. The cleared lysate obtained by centrifugation and filtration (0.45 μm filter) was incubated with 3 ml Talon resin for 1 h. The affinity matrix was applied to a polypropylene column, washed extensively with Talon-wash buffer and eluted with Talon-elution buffer.

3.2.5.4 Purification with Strep-Tactin

The StrepII-tag is a peptide sequence that binds to the biotin binding site of streptavidin. StrepII fusion proteins are purified with Strep-Tactin, an optimized streptavidin mutant. The elution is carried out by the addition of the biotin analog desthiobiotin.

The fusion protein with a StrepII-tag was loaded on a self-packed 4 ml Strep-Tactin MacroPrep polypropylene column equilibrated with buffer W. The column was washed extensively with the same buffer, and subsequently the protein was eluted using buffer W supplemented with 2.5 mM desthiobiotin.

3.2.5.5 Purification of His-tagged proteins under denaturing conditions

Binding of His-tag fusion proteins to Ni-NTA does not require proper folding of the protein. Thus, insoluble proteins can be purified under denaturing conditions.

Cells were lysed in His-lysis buffer and the pellet obtained by centrifugation at 46,000x g for 20 min was resuspended in denaturing buffer. The suspension was incubated for 1 h and centrifuged 20 min at 46,000x g, and the supernatant was loaded on 2 ml Ni-NTA resin in a polypropylene column. The column was washed with denaturing buffer, pH 6.3, and protein was eluted with 5 ml denaturing buffer, pH 4.5.

3.2.6 Determination of protein concentration

To determine the concentration of protein preparations, a UV spectrum of the samples was recorded. The absorbance at 280 nm was used to calculate the protein concentration with Beer's law based on the molar extinction coefficient (ϵ) calculated with ProtParam [71].

Beer's law: $I = I_0 \cdot 10^{-\epsilon \cdot c \cdot d}$ or $A_\lambda = \epsilon_\lambda c d$ (Equation 3.1)

ϵ_λ : the molar extinction coefficient [$\text{M}^{-1} \text{cm}^{-1}$] at a given wavelength

c: concentration [M].

d: path length [cm]

Protein	ϵ_{280} [$M^{-1} \text{ cm}^{-1}$]	A_{280} at 1 mg ml ⁻¹
His-Tpc6B	10,810	0.60
Tpc6B	10,818	0.61
His-Bet3-StrepII	17,000	0.73
His-Tpc5	16,500	0.69
Mum2	18,490	1.1
His-Bet3:Tpc6B	21,620	0.54
His-Bet3:Tpc6A	26,030	0.65
His-Bet3:Tpc6B:Mum2	40,110	0.72
His-(Bet3:Tpc6B:Mum2: synbindin)	71,630	0.80

Table 3.14: Molar extinction coefficients of recombinant TRAPP subunits and complexes used for determination of protein concentration.

3.2.7 Tag removal

To cleave the affinity tag from the recombinant protein, specific recognition sites for proteases are introduced in the expression constructs. The His-tag of pQTEV can be removed with tobacco etch virus (TEV) protease, pGEX-6P1 contains a PreScission protease cleavage site. Elution fractions from affinity purification containing recombinant protein were incubated with the required protease at a ratio of 20:1 to 100:1 (fusion protein:protease, w/w) at 4 °C until cleavage was complete (usually over night).

To separate cleaved protein from the tag and uncleaved protein, TEV digest reactions were dialysed against His-lysis buffer and loaded onto a Ni-Poros column with a VISION chromatography system. Unbound fractions were collected and further purified. For cleavage of the GST tag from GST-Mum2, PreScission digested samples were loaded on a HiTrap S cation exchange column equilibrated with 50 mM Tris pH 7.5, 1 mM DTT using a Pharmacia FPLC system. Bound Mum2 was eluted with a 0 to 1 M linear NaCl gradient in same buffer at approximately 0.5 M NaCl.

3.2.8 Gel-filtration chromatography

Gel-filtration, also known as size-exclusion chromatography, relies on the separation of particles based on their size. The column material is composed of inert polymer beads with a

defined pore diameter. When applied to such a column, proteins will be separated according to their size and shape. With smaller molecules being able to enter the pores, these travel a longer way through the column and will be eluted later than bigger particles. Every column has a characteristic void volume, that is the minimum volume a big particle needs to pass through without entering any pore. The column volume gives the total amount of buffer that is required to equilibrate the system.

Gel-filtration columns can be calibrated by determining the elution volume of standard proteins. A linear relation exists between the logarithm of the molecular weight of the compounds and their elution volume. Thus, the molecular weight of a sample protein can be calculated based on the elution volume observed in gel-filtration chromatography.

Gel-filtration experiments were performed with Pharmacia FPLC systems or Äkta Explorer, and the size-exclusion column was equilibrated with 2 column volumes of buffer. In this study, Superdex 75 and Superdex 200 columns were used, that differ in their pore sizes and thus have different optimal separation ranges (3-70 kDa and 10-600 kDa, respectively). The sample volume was 1-2 ml for 16/60 columns and up to 5 ml for columns with dimensions of 26/60 (diameter in mm/length in cm). The elution profile was monitored measuring the absorption at 280 nm and peak fractions were analyzed with SDS-PAGE.

3.2.9 Sodium dodecylsulfate polyacrylamide-gel electrophoresis (SDS-PAGE)

Discontinuous SDS polyacrylamide-gel electrophoresis (SDS-PAGE) was used to determine the purity of protein samples. The gels were produced by co-polymerization of acrylamide with the crosslinker N,N'-methylenebisacrylamide in the presence of the radical starter ammonium peroxydisulfate (APS) and the catalyst tetramethylethylenediamine (TEMED). Variations in the concentration and the ratio of both monomers regulate the crosslinking and thus the pore size of the gel. SDS is an anionic detergent that denatures proteins and binds to proteins with a constant ratio of 1.4:1. Thereby the charges of the proteins are masked and their migration velocity in an electric field is approximately proportional to the logarithm of their molecular mass. Before entering the separation gel, proteins are focused in a stacking gel with wide pores at pH 6.8. The comparison to a marker lane with proteins of known size allows an estimation of the size of the sample.

Prior to SDS-PAGE, samples were mixed with SDS-sample buffer and boiled for 5 min. Electrophoresis was carried out with PAGE-buffer at 120 V (stacking gel) for 15 min and 60-90 min at 180 V (separation gel).

3.2.10 Staining of PAGE gels

For staining with Coomassie Brilliant Blue, gels were boiled 30 s in Coomassie stain solution. The gel was rinsed with water, then boiled for 30 s in destain solution and shaken at room temperature until it was completely destained.

Silver staining was done according to the protocol by Nesterenko *et al.* [72]. The gel was fixated for 5 min in fixation solution, rinsed trice, washed 5 min and rinsed three times again with water. After pretreatment for 5 min in 50% acetone and 1 min in reducing solution the gel was rinsed with water and impregnated with silver stain solution for 8 min. After rinsing twice with water, the gel was developed with development solution until bands started to appear (usually 10 to 30 s) and stopped with 1% glacial acetic acid in water.

3.2.11 Concentration of protein samples

Protein solutions were concentrated with ultrafiltration devices Amicon Ultra available with 5 kDa, 10 kDa and 30 kDa molecular weight cut-off. Samples were loaded onto the filtration membrane and centrifuged at 4 °C 4000x *g*. While water and buffer molecules can pass the membrane, protein is retained and thus concentrated.

3.2.12 Circular Dichroism

Circular dichroism allows to estimate the secondary structure content of proteins and can be used to investigate the folding state of a protein. The method is based on chirality of biological molecules, which leads to different extinction coefficients for left- and right-circularly polarized light in optically active molecules. This difference is measured as ellipticity θ_λ :

$$\tan \theta_\lambda = \frac{I_R - I_L}{I_R + I_L} \quad (\text{Equation 3.2})$$

$I_{R/L}$ are the intensities of the left- and right-circularly polarized light after passing the sample.

With Beer's law (Equation 3.1) we get an approximation for small ellipticities:

$$\theta_\lambda = \ln 10 \cdot \frac{180^\circ}{4\pi} \cdot (\varepsilon_L - \varepsilon_R) \cdot c_M \cdot d \quad [^\circ] \quad (\text{Equation 3.3})$$

$\varepsilon_{R/L}$: molar extinction coefficient left- and right-circularly polarized light [$\text{M}^{-1}\text{cm}^{-1}$]

c_M : concentration [M]

d : pathlength [cm]

For historical reasons, the molar ellipticity $[\theta_M]_\lambda$ (Equation 3.4) is commonly used in CD spectroscopy:

$$[\theta_M]_\lambda = \frac{\theta_\lambda \cdot M}{c_m \cdot d \cdot 100} \quad [^\circ \cdot \text{cm}^2 \text{ dmol}^{-1}] \quad (\text{Equation 3.4})$$

c_m : concentration [g cm^{-3}]

d : pathlength [dm]

M : molecular mass [g mol^{-1}] of the optically active residue, which is 110 g mol^{-1} (the average amino acid mass) in the case of proteins.

Besides the intrinsic optical activity of the individual amino acids, proteins give further CD-signals that arise from the coupling of chromophores in secondary structure elements such as α -helix and β -sheet, but also from random coils [73]. These elements give rise to characteristic spectra, so that the CD spectrum of a protein allows to estimate the relative presence of the different secondary structure elements.

To record CD spectra of Bet3, Tpc6B and Tpc5, protein samples were diluted to 0.1 - 0.05 mg ml^{-1} and dialysed against PBS. Three spectra were accumulated with a Jasco J720 spectropolarimeter at 20 °C from 260 nm to 200 nm with a 0.1 cm pathlength cuvette.

Melting curves of human Bet3 purified from yeast and chemically depalmitoylated Bet3 were recorded with a Jasco J720 spectropolarimeter with temperature control. Protein samples were diluted to $\sim 0.1 \text{ mg ml}^{-1}$ and buffer was exchanged to PBS. Measurements were carried out at 222 nm with a 0.2 cm pathlength cuvette. Unfolding was monitored following the decrease of ellipticity during heating of the sample $0.5 \text{ }^\circ\text{C min}^{-1}$ from 20 to 80 °C.

3.2.13 Dynamic light scattering

Dynamic light scattering is used to estimate the size of protein particles in solution. If a colloidal dispersion is irradiated with light of a wavelength much larger than the size of the particles to be measured, light is scattered uniformly in all directions (Rayleigh scattering). The particles undergo Brownian motion, which is dependent on their size. As a consequence, the distance between particles varies over time, leading to changes in interference of scattered light, thus fluctuations in the scattering. These fluctuations can be measured when coherent and monochromatic (laser) light is used, and allows the determination of the diffusion coefficient D of the particle. With the Stokes-Einstein equation the particle size, i.e. the hydrodynamic radius R , is calculated.

$$R = \frac{6\pi\eta D}{kT} \quad (\text{Equation 3.5})$$

η : viscosity of the medium

3.3 Protein crystallography

Besides nuclear magnetic resonance (NMR), protein crystallography is the most powerful method to determine the three-dimensional structure of biological macromolecules, i.e. nucleic acids, lipids, saccharides and proteins, but also complexes of these molecules with ligands that might be any chemical compound.

The principle of X-ray crystallography can be clarified in analogy to the function of a light microscope. To obtain a magnified picture of e.g. a bacterial cell, the object is irradiated with visible light (400-700 nm), which is diffracted by the object. The diffracted light is collected by a system of lenses, which will produce a magnified picture. The wavelength of the used light has to be in the order of the distances that are to be observed, thus visible light is suitable for the investigation of single cells.

To resolve individual atoms, as required for determination of a molecular structure, X-rays are used because their wavelength (1-1.5 Å) is approximately the distance between covalently linked atoms. Only the diffraction of X-rays by an ordered arrangement of macromolecules in a crystal gives a detectable signal, which explains the need for protein crystallization. The diffracted X-ray beams cannot be collected by a physical lens system, so that the diffraction pattern has to be recorded and the picture has to be calculated using Fourier transformation, which is the mathematical description of diffraction.

3.3.1 Crystallization

Finding the right conditions for the growth of protein crystals is still a major bottleneck in X-ray crystallography. The principle of crystallization is to slowly reduce protein solubility by increasing the precipitant and protein concentrations. Under the right condition a supersaturated state can be reached, where few nuclei form and grow to become crystals. If the conditions are not optimal, the protein will precipitate or form microcrystals at too high concentrations, or the drop may stay clear if protein and precipitant concentration are too low. This can be illustrated with a phase diagram (Figure 3.1). Depending on protein and precipitant concentration the system is in an undersaturated or a supersaturated state. Crystals will not grow but dissolve in the undersaturated region. For supersaturation it can be differentiated between the labile state where nuclei can spontaneously form and grow and the metastable state where nuclei can grow but not form. Nucleation and crystal growth in the supersaturated phase are always in competition with amorphous precipitation, which will occur when protein and/or precipitant concentration are too high.

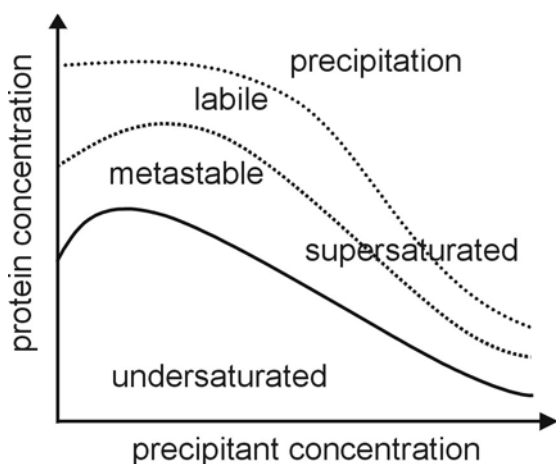


Figure 3.1: Phase diagram showing the solubility curve (solid) of a protein depending on protein and precipitant concentration. The supersaturated phase can be separated into metastable and labile areas, where crystal nucleation and growth can occur, and an area with precipitation. The depicted example is the special case of a protein showing a salting in effect (after [3]).

The most commonly used technique for growing crystals is the vapor-diffusion method. Small volumes of precipitant solution and protein sample are mixed and thus both diluted. The drop is then equilibrated against a large reservoir filled with the precipitant solution in a closed system. The most volatile component (usually water) will evaporate from the drop and condensate at the reservoir. Thus, the volume of the droplet will be reduced and protein and precipitant concentration will slowly increase. Volatile organic solvents, if present in the precipitant solution, will diffuse from the reservoir to the drop until equilibrium is reached. In this case, the protein solution in the drop decreases, whereas the precipitant increases. Vapor-diffusion can be done e.g. with the hanging-drop or the sitting-drop method. The hanging drop is mixed on a cover slide that is used upside down to cover the reservoir well. Silicon grease is used to seal the cover. The sitting drop is mixed in an elevated pit above the reservoir and the well will also be sealed.

The success of crystallization is dependent on the quality of the sample preparation (homogeneity) and the setup of the crystallization experiment. Crystallization space is defined by numerous variables that can be optimized, such as temperature, solvent, precipitant concentrations, pH, additives (e.g. ligands, cofactors, salts) and the kind of precipitant. The most common precipitants are PEGs (polyethylene glycols), salts (especially ammonium sulfate, Na/K phosphate and sodium chloride) and organic reagents (mainly 2-methyl-2,4-pentanediol, MPD). The best way to screen the multi-dimensional crystallization space is with sparse matrix screens. These screens try to cover the whole range of crystallization conditions and are formulated on the basis of precipitant solutions that have been successfully used in crystallization trials before. Once initial crystallization conditions are found, a systematic optimization with grid screens is required, where each parameter is varied so that the best crystals possible can be grown.

For the collection of high-resolution data, high-intensity X-ray synchrotron radiation is used. To avoid radiation damage of the crystals, they have to be vitrified and cooled in a liquid

nitrogen stream. This also enhances the signal-to-noise ratio in data collection because the atomic motion is reduced at such low temperatures. The formation of ice crystals that will interfere with the diffraction pattern and might destroy the protein crystal has to be prevented by the use of optimized cryo-conditions. If the mother liquor the crystal has grown in is not suitable, cryo-protectants (e.g. glycerol, low molecular weight PEGs, MPD) have to be added to the solution. The crystal has to be transferred into the cryo-solution and can then be frozen.

Applications

Crystallization experiments for this study were carried out in 96-well format at 20 °C by the sitting-drop vapor-diffusion method using a semi-automated dispensing system [74]. Crystal Quick crystallization plates were filled with 400 µl precipitant solution in the reservoir and droplets containing 400 nl of each protein solution and precipitant were set up using a Hydra-Plus-One or Hydra-II robot. The purified protein samples were applied to the initial crystal screens Hampton, PEG_Ion, Index_HT, Salt_HT, HuMag and ProComp (see appendix B). These screen formulations are based on the commercially available screens from Hampton Research and were produced with a Lissy XXL robot. Initial crystal hits were subsequently refined with grid screens, composed by hand and applied with the Hyrda robots. Crystallization setups were digitally photographed and evaluated using the program OBSERVATION (developed by M. Höschen). Cryo-conditions for the freezing of crystals were obtained by the addition of glycerol. Crystals were transferred with a nylon loop onto a pin into cryo-solution, soaked for 1 min, mounted in a nylon loop and flash-frozen in liquid nitrogen.

3.3.2 Collection of diffraction data

Any crystal constitutes of small building blocks, called unit cells, that are arranged by translation in an ordered array in the same orientation. A unit cell defines the crystal coordinate system by three edges (a , b , c) and three angles (α , β , γ), that can all be different or obey some restrictions depending on the crystal system.

If the content of the unit cell possesses internal symmetry, the cell can be further dissected into asymmetric units. The content of an asymmetric unit is the smallest entity that is sufficient to build up the complete unit cell by applying the symmetry operations. A 2-fold axis reduces the asymmetric unit to half of the unit cell, a 3-fold axis to a third etc., and symmetry elements in different directions multiply. To the same extent the degrees of crystal rotation required for the collection of complete data sets are reduced. In a protein crystal, only rotational symmetry (rotation or screw axes) can occur, because due to the chirality of the

amino acids no mirror planes and inversion centers are possible. That reduces the number of possible space groups from 230 to 65, which are listed in the International Tables for Crystallography [75].

Within each crystal, sets of equivalent, parallel lattice planes can be define based on their orientation in the unit cell. The Miller indices h , k and l define how often a set of parallel lattice planes intersects with the unit cell edges a , b , c . Lattice planes are a helpful concept to understand scattering of X-rays by a crystal. Bragg showed that the diffraction by a crystal can be described like the diffraction by the sets of lattice planes. The diffracted beams from equivalent lattice planes will only result positive interference if Bragg's law is fulfilled:

$$2d_{hkl} \sin \theta = n\lambda \quad (\text{Equation 3.6})$$

d_{hkl} : distance of lattice planes

θ : diffraction angle

λ : wavelength

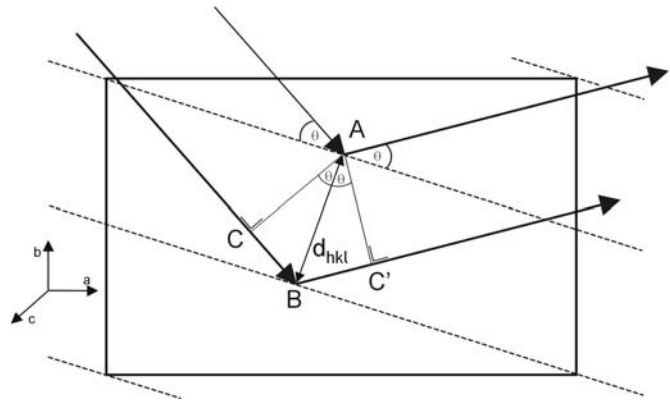


Figure 3.2: Bragg's law for the diffraction of X-rays on the lattice planes of a crystal

Figure 3.2 shows as an example the reflection at the (120) plane. The angle θ has to be so that the distance $|CB| + |BC'|$ (given by $2d_{hkl} \sin \theta$) equals an integer multiple of the wavelength λ to have positive interference after diffraction. If the waves were not in phase, for the diffracted wave from each plane a parallel plane will exist that produces a wave with destructive interference that will cancel out each other. The minimal distance between lattice planes defines the maximal resolution of a diffraction experiment and has the theoretical limit of $d_{\max} = \lambda/2$. In practical application, the quality of the crystal (size and packing) further limits the resolution.

The diffracted X-rays from one set of lattice planes will give rise to one reflection of the diffraction pattern. Thus, the reflections are indexed using the same indices $h k l$ from the lattice planes. As the values of $h k l$ rise, spacings between lattice planes decreases, the angle θ increases and reflections at higher resolution are observed. To illustrate the direction of diffraction by a crystal, the reciprocal space can be constructed. It is defined by the edges a^* , b^* and c^* ($1/a$, $1/b$ and $1/c$ for orthorhombic unit cells) and the angles α^* , β^* and γ^* (all 90° in orthorhombic unit cells). A sphere with the radius $1/\lambda$ around the crystal passing through the origin of the reciprocal space is called Ewald's sphere. An incoming X-ray wave through

the center (C) of the sphere and the origin of reciprocal space (O) will be scattered, and break through the sphere at each lattice point (P) that is located on the sphere (Figure 3.3). The difference vector \mathbf{S} between incoming (\mathbf{s}_0) and scattered (\mathbf{s}) beam is called diffraction vector, pointing in reciprocal space from the origin to the lattice point on Ewald's sphere.

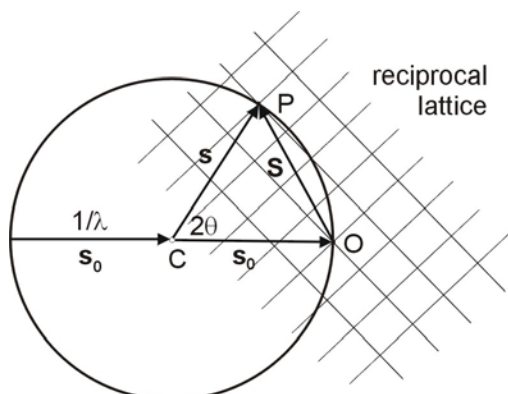


Figure 3.3: A sphere with the radius $1/\lambda$ passing through the origin of the reciprocal space (O) is called Ewald's sphere. The incoming X-ray wave \mathbf{s}_0 will be scattered (\mathbf{s}) at the crystal in the center (C) and break through the sphere at the lattice point (P) that is located on the sphere (after [1]).

Thus, the diffraction pattern is a projection of the reciprocal lattice points that lie on Ewald's sphere at a given orientation of the crystal in the beam. As the crystal is rotated, the reciprocal lattice is moved through Ewald's sphere and more reflections $h k l$ are measured. Because the $h k l$ plane equals the $-h -k -l$ plane, the intensity of $h k l$ is the same as that of $-h -k -l$ (Friedel's law). Thus, the diffraction image is centro-symmetric even though the crystal is not and the data that has to be measured is cut by half.

From the reciprocal cell dimension observed in the diffraction pattern the dimensions of the real unit cell can be calculated. In addition, the symmetry of the unit cell is preserved in the diffraction pattern and systematic absences of Bragg reflections occur in the diffraction pattern that help identifying the space group.

Applications

Data for the structure determination of Tpc6B and the Bet3:Tpc6B complex were collected at beam-lines BL14.1 and BL14.2 at BESSY, Berlin [76]. Diffraction patterns were recorded using a Mar345 image plate or Mar165ccd (charged-coupled device) camera. Data were indexed with DENZO [77] or XDS [78] and the unit cell parameters and space groups were assigned. Complete data sets were recorded according to the space groups determined.

3.3.3 Data processing

To obtain a complete data set, that is a measurement of all reflections $h k l$, a data collection strategy is employed based on the orientation and space group of the crystal. The diffraction patterns are indexed, that is h , k and l are assigned to the individual reflections. The same reflection might be recorded several times on different images as the corresponding reciprocal lattice point might lie on Ewald's sphere at different orientations of the crystal. This can be

used to scale the individual images, as the intensities for $h k l$ (and $-h -k -l$) should be the same in each frame. Also, pairs of reflections related by crystallographic symmetry (Bijvoet pairs) can be averaged to improve the accuracy of data. The scaling will compensate for some errors arising from crystal damage during measurement, X-ray absorption and scattering or anisotropy of the crystal.

Because the reciprocal lattice points are not one-dimensional, but have to be considered being spheres, they can pass Ewald's sphere completely or only partially at a given angle and oscillation range of the crystal. During post-refinement partial reflections can be discarded if the same $h k l$ is recorded fully in another frame, or a partiality value is assigned that allows an estimation of the full intensity of the given reflection. The outcome of the data reduction is a set of unique structure factor amplitudes.

Applications

For scaling, the programs SCALEPACK [77] or XDSSCALE [78] were used. Data from XDSSCALE had to be converted with XDSCONV [78] for further processing with CCP4 programs [79]. The quality of the data collection is represented by the R_{sym} factor.

$$R_{sym} = \frac{\sum_{hkl} \sum_i |\overline{I(hkl)} - I_i(hkl)|}{\sum_{hkl} \sum_i I_i(hkl)} \quad (\text{Equation 3.7})$$

Here $I_i(hkl)$ is the intensity of a given measurement and $\overline{I(hkl)}$ is the average of that reflection from all measurements. The sums are over all individual measurements of the same reflection i and over all reflections (hkl).

3.3.4 Determination of electron density

The electron density in the unit cell can be described as a three-dimensional Fourier series of three-dimensional waves. A reflection of the diffraction pattern is also a wave and can be described as structure factor $\mathbf{F}(hkl)$ that is a Fourier series of atomic scattering factors f_j . Thus, each atom j in the unit cell contributes to each structure factor.

$$\mathbf{F}(hkl) = \sum_j f_j e^{2\pi i(hx_j + ky_j + lz_j)} \quad (\text{Equation 3.8})$$

h, k, l : reflection indices in reciprocal space

x_j, y_j, z_j : coordinates of atom j in real space

Instead of summing over all atoms in the unit cell, the integral over the electron density at all volume elements around (xyz) of the electron density can be calculated.

$$\mathbf{F}(hkl) = \int_V \rho(xyz) e^{2\pi i(hx + ky + lz)} dV \quad (\text{Equation 3.9})$$

This mathematical description shows that a real space wave can be converted into a wave in reciprocal space using a Fourier transform. The reverse is also true, so $\rho(xyz)$ is the Fourier transform of $\mathbf{F}(hkl)$, which allows the calculation of electron density from structure factors.

$$\rho(xyz) = \frac{1}{V} \sum_h \sum_k \sum_l \mathbf{F}(hkl) e^{-2\pi i(hx+ky+lz)} = \frac{1}{V} \sum_h \sum_k \sum_l |F(hkl)| e^{i\alpha(hkl)} e^{-2\pi i(hx+ky+lz)}$$

(Equation 3.10)

Because $h k l$ are discrete lattice points, the function is a sum rather than an integral. The structure factors are composed of an amplitude and a phase contribution. Whereas the structure factor amplitudes can be derived from the intensities in the diffraction pattern (Equation 3.11), phase information is lost and has to be obtained by methods discussed below.

$$\sqrt{|I(hkl)|} \sim |F(hkl)|$$

(Equation 3.11)

3.3.4.1 Single wavelength anomalous dispersion (SAD) phasing

Anomalous scattering occurs at the absorption maximum of an element, when electrons are elevated to higher states and re-emit radiation when falling back to the initial energy. This process entails a phase shift of the scattered wave, thus an imaginary component is added to the total atomic scattering factor.

$$f_i(\theta, \lambda) = f^0(\theta) + \Delta f(\lambda) + if''(\lambda) = f' + if''$$

(Equation 3.12)

f^0 : normal atomic scattering, angle-dependent

$\Delta f, f''$: real and imaginary anomalous dispersion correction, wavelength-dependent

The imaginary component of the scattering is always positive. This leads to the breakdown of Friedel's law, illustrated by Argand diagrams (Figure 3.4)

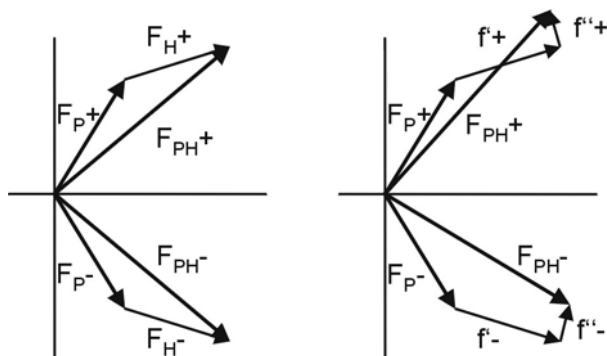


Figure 3.4: Argand diagrams for normal scattering obeying Friedel's law (left) and anomalous scattering, where Friedel's law no longer holds (right).

These anomalous differences between Friedel mates can be used to determine the coordinates defining a sub-structure of the anomalous scatterers with Patterson methods.

A peak in Patterson space will occur at a vector \mathbf{u} that relates two atoms \mathbf{r} and $\mathbf{r}+\mathbf{u}$ in real space. This function will be zero for most points, unless electron density is found at both coordinates.

$$P(\mathbf{u}) = \int_{\mathbf{r}} \rho(\mathbf{r}) \times \rho(\mathbf{r} + \mathbf{u}) d\mathbf{v} \quad (\text{Equation 3.13})$$

An equivalent expression for the Patterson function is

$$P(uvw) = \frac{1}{V} \sum_{hkl} |F(hkl)|^2 e^{2\pi(hu+kv+lw)} \quad (\text{Equation 3.14})$$

which is an expression of coordinates in Patterson space that is dependent only on structure factor amplitudes and does not require any phase information. The Patterson map of a protein is too crowded, but for a small subset of anomalous scattering atoms (or heavy atoms in isomorphous replacement) real space coordinates ($x y z$) can be derived from the difference Patterson peaks ($u v w$).

In SAD phasing, the Bijvoet differences are used to calculate a difference Patterson map with $|F(hkl)| = |F^+| - |F^-|$. The coordinates obtained are used to calculate the structure factors of the anomalous scattering atoms subset. With this information and the knowledge of f'' (only dependent on wavelength), initial phases can be estimated.

$$\mathbf{F}_P = \mathbf{F}_{PH}^- - \mathbf{F}_H - \mathbf{F}'' = \mathbf{F}_{PH}^+ - \mathbf{F}_H - \mathbf{F}'' \quad (\text{Equation 3.15})$$

As illustrated by a Harker construction [80], the different amplitudes from the Friedel pairs and the contribution of the anomalous scatterer will give rise to two possible phases. The phase ambiguity has to be overcome with phase improvement methods like density modification and, if applicable, non-crystallographic symmetry (NCS) averaging.

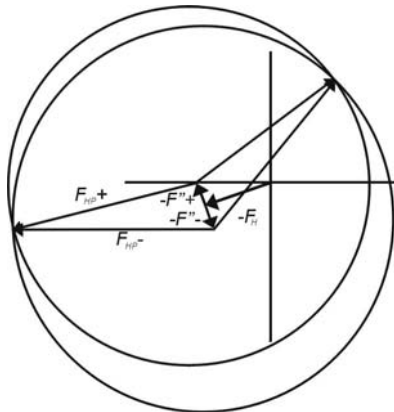


Figure 3.5: Harker construction for initial phase determination from SAD data collection. The phases are underdetermined resulting in phase ambiguity.

SAD experiments have to be carried out at synchrotron beam-lines with tunable wavelength. With a fluorescence wavelength scan, the absorption maximum of the atomic scatterer in the protein environment has to be determined. At the peak wavelength, anomalous scattering is maximal, yielding optimal data to detect anomalous differences.

Applications

For anomalous data collection a fluorescence scan of the SeMet Tpc6B crystals at the selenium edge (0.979 Å) was performed, and the optimal wavelength and the atomic scattering

factors were determined with the program chooch [81]. The program SOLVE [82] was used to automatically solve the Patterson function for determination of the coordinates of the anomalous scatterers' subset and calculation of initial phases. In combination with RESOLVE [83], that carries out statistical density modification and automated model building, a initial model was obtained that could be further improved by manual model building and structure refinement.

3.3.4.2 Molecular replacement

If a homologous structure is known or a model is available for the protein structure to be determined, molecular replacement can be used to generate initial phases. This is especially suitable for the structure determination of proteins with different ligands, where only minor parts in the structure differ.

If the model was derived from a non-isomorphous crystal, the initial task is to place the model in the right orientation and at the correct position of the unit cell of the measured crystal. The problem is dissected into two different searches. The rotation function identifies the correct orientation in the absence of translational contribution by comparison within a sphere of Patterson space that should only includes intra-molecular cross-vectors. Therefore, an orientation of the model is searched that gives a Patterson map as similar as possible to the Patterson map of the collected data. The agreement is evaluated with a scoring function

$$S = \int_{r_1}^{r_2} P_{model} \times P_{data} dr \quad (\text{Equation 3.16})$$

that is maximal when the Patterson maps of the model (P_{model}) and the data (P_{data}) within a shell around the origin defined by the radii r_1 and r_2 match best.

The best orientation(s) are fixed and subsequently used for a translational search. The limits of the shell (r_1 and r_2) are now chosen so that inter-molecular cross-vectors of the Patterson function are included in the search. In addition, structure factor amplitudes can be calculated based on the model and compared to $|F_{obs}|$ using the crystallographic R -factor (Equation 3.21). The best agreement between the Patterson maps (high scoring function) and structure factor amplitudes (low R -factors) gives the best position of the model. Phases α_{calc} derived from this model are used with $|F_{obs}|$ to calculate initial electron density according to Equation 3.10.

Applications

These principles are implemented in the program MOLREP [84], that was used for molecular replacement in this study. For the structure of the Bet3:Tpc6B complex, models of the subunits alone were known and could be used as search models. First positions for the Bet3

monomer (PDB 1SZ7) were searched and fixed, and subsequently Tpc6B monomers (PDB 2BJN) were placed in the asymmetric unit. This led to the identification of two heterodimers per asymmetric unit.

3.3.5 Model building

The initial models from automated model building (3.3.4.1) or molecular replacement (3.3.4.2) have to be modified and improved manually. Therefore, weighted electron density maps are calculated that facilitate the interpretation of the data and the comparison with current model. The $2F_o - F_c$ map

$$\rho(xyz) = \frac{1}{V} \sum_h \sum_k \sum_l \|2 \cdot F_{obs} - F_{calc}\| e^{-2\pi i(hx+ky+lz)+i\alpha_{calc}} \quad (\text{Equation 3.17})$$

gives a simple electron density map (usually contoured at 1σ) that enhances differences between measured and calculated structure factor amplitudes and thus reduces model bias.

The $F_o - F_c$ map

$$\rho(xyz) = \frac{1}{V} \sum_h \sum_k \sum_l \|F_{obs} - F_{calc}\| e^{-2\pi i(hx+ky+lz)+i\alpha_{calc}} \quad (\text{Equation 3.18})$$

is called difference electron density map and is displayed at lower contour levels (usually 3σ). This reveals where model still has to be built (peaks at positive difference density) or model has been built wrongly (peaks at negative difference density).

Applications

Weighted density maps were calculated with FFT [79] and displayed in the programs O [85] or with a routine in COOT [86]. The visualization programs O and COOT were used to manually build or re-build the model. At advanced stages of model building, water molecules, ligands and, in case of Tpc6B, alternative conformations were built in positive peaks of the difference electron density map. This process was supported by automated model building and water search routines that are implemented in the programs ARP/wARP [87] or COOT [86].

3.3.6 Refinement

The model building process in real space is monitored and supported by computational refinement in reciprocal space to improve the agreement of F_{obs} and F_{calc} . This problem is treated as the energy minimization of the function

$$E_{total} = E_{stereo} + E_{xray} = E_{stereo} - s \sum_{hkl} \log\{p |F_{obs}(hkl)|; p[\mathbf{F}_{calc}(hkl)]\} \quad (\text{Equation 3.19})$$

that is divide into a stereochemical term E_{stereo} and an X-ray term E_{xray} .

The stereochemical term assigns penalties for all deviations from standard bond lengths, bond angles, group planarities, chiral centers, nonbonded contacts and torsion angles, and these functions are minimized by least-squares or maximum likelihood methods. In addition, constraints (fixed parameters) may be imposed on the model. It has been shown that the X-ray term can be minimized by a maximum likelihood function to reduce the differences between observed and calculated structure factor amplitudes, which gives considerably better results than least-squares methods. The X-ray term is scaled in respect to the stereochemical term with the scaling factor s , that allows to emphasize either term, depending on the quality of the data.

The dynamic mobility of an atom can be refined as the positional displacement. The B- (or temperature-) factor describes the statistical motion of an atom by an isotropic sphere with the radius r (r^2 is the mean square displacement).

$$B = 8\pi^2 r^2 \quad (\text{Equation 3.20})$$

The B-factor is included in the calculation of structure factors as a weighting term that reduces the contribution of atoms with high B-factors. Thus, a high B-factor of an atom might also indicate an error in the model.

An anisotropic refinement of atomic displacement can be carried out with TLS (translation, libration, screw-motion) parameters assigned to individual groups of the model. This requires fewer parameters than a full anisotropic atomic B-factor refinement and is at a subdomain level suitable for data with 1.5 Å to 2.5 Å maximal resolution. Residues of the molecule are grouped and treated as a rigid body with 6 translation, 6 libration and 8 screw-motion degrees of freedom in displacement.

The quality of the model in respect to its agreement with the original data is given by R_{work} and R_{free} .

$$R_{work / free} = \frac{\sum_{hkl} \left| |F_{obs}| - |F_{calc}| \right|}{\sum_{hkl} |F_{obs}|} \quad (\text{Equation 3.21})$$

where R_{free} is calculated for a test set (usually including 5% of the data) that is not refined and R_{work} is calculated for the remaining reflections that are included in the refinement.

A further criterion to judge a protein model is the abundance of stereochemical parameters, that are also optimized during refinement. The root-mean-square deviations (rmsd) from standard bond lengths, angles and planarity should be within a reasonable range. Furthermore, the torsion angles between the peptide planes at the C α atom of an amino acid are restricted to defined combinations, summarized in the Ramachandran plot.

Applications

For both structures described in this study, refinement was carried out without a test set containing 5% of unique reflections that are not included in refinement and define R_{free} . The remaining reflections were refined with REFMAC5 [88] using maximum likelihood methods. Refinement included positional, B-factor and TLS group refinement. TLS groups were defined after examination of B-factor plots, so that one TLS group includes all residues between two local B-factor minima and contains more than 5 residues.

The stereo parameters were monitored using PROCHECK [89]. Severe violations of stereochemistry (e.g. cis-peptides, outliers in the Ramachandran diagram) were subsequently corrected with the model building programs. After each round of model building, refinement was carried out to evaluate the success of structure modification. The indication for this are reduced R -factors and a decreased difference between R_{free} and R_{work} as well as improved stereochemistry. If these criteria were not fulfilled, changes were rejected.

3.4 Biochemical studies

3.4.1 Cell culture

HEK293 cells were grown in DMEM (Dulbecco's Modified Eagle's Medium) supplemented with 10% fetal calf serum, penicillin/streptomycin (100 U ml⁻¹/0.1 mg ml⁻¹) and sodium pyruvate (1 mM). Cells were fed twice a week and split when they became confluent in the culture plate. For splitting, medium was removed and cells were washed with PBS. After addition of 1 ml trypsin/EDTA solution, plates were incubated at 37 °C for 1 min and the cells were resuspended in 10 ml medium. New culture plates were seeded at ratios from 1:3 to 1:10 for continuous passages. For transfections, 2 x 10⁶ cells were seeded per 10 cm Petri dish in 10 ml medium 24 h prior to the experiment.

3.4.2 Transient expression in eukaryotic cells

HEK293 cells were transfected with encoding plasmids by calcium precipitation. For one 10 cm culture plate 10 µg DNA were mixed with 38 µl CaCl₂ (2 M) in 250 µl water. The mixture was pipetted into 300 µl 2x HBS and incubated 15 min at room temperature. Insoluble calcium phosphate crystals form, which also contain plasmid DNA. Reactions were then pipetted to the cell. The precipitate is taken up by the cells *via* endocytosis, leading to transient expression of the encoded genes.

After 24 h cells were lysed in CoIP buffer containing protease and phosphatase inhibitors.

3.4.3 Association studies

Proteins were precipitated with α-flag or α-myc antibodies and Protein G-Sepharose or α-HA-affinity matrix. To each sample, 1 µl of antibody was added and reaction was incubated overnight at 4 °C on a rotating wheel. 10 µl Protein G-Sepharose were added and incubation was continued for 1 h. Of the α-HA affinity matrix, 10 µl were added instead of antibody and protein G-Sepharose, and samples were incubated for 2 h. The immuno-precipitations (IP) were centrifuged at 1000x g for 1 min and washed 5 times with CoIP buffer, resuspended in 2x PAGE buffer and subjected to SDS-PAGE and Western blot analysis.

For His-pulldowns, 12 µg of recombinant protein was pre-incubated with 25 µl Talon resin in 800 µl CoIP buffer containing 0.1% bovine serum albumin for 8 h. Beads were washed and incubated with lysates from HEK293 cells expressing epitope-tagged proteins for 14-16 h. The resin was centrifuged at 1000x g for 1 min and washed 3 times with CoIP buffer. Samples were then subjected to SDS-PAGE and Western blot analysis.

Crosslinking experiments were performed with 0.1 mM glutaraldehyde for 2 h after pre-incubation of protein mixtures (protein concentration 50 μ M each) over night. Samples were analysed by SDS-PAGE and Coomassie staining.

3.4.4 Western blot

Before the immunodetection, proteins were transferred from polyacrylamide gels onto nitrocellulose or polyvinylidene fluoride (PVDF) membranes [90]. PVDF membranes have to be activated by soaking in methanol prior to usage. The transfer was performed for 1 h with a semi-dry blotting apparatus at 60 mA per 6 x 9 cm gel with filter paper and membranes soaked in semi-dry blotting buffer.

3.4.5 Immunodetection

The detection of proteins immobilized on membranes was done with specific antibodies against the epitope tags. The membrane was blocked with PBS-T with 3% BSA to saturate unspecific binding sites. Primary antibodies diluted in PBS-T with 1.5% BSA (α -flag 1:6000, α -myc 1:2000, α -HA 1:1000) were incubated with the blocked membranes for 1 h at room temperature or over night at 4 °C. The primary antibody solutions were collected and re-used. After washing three times for 15 min with PBS-T, the membrane was incubated for 1 h at room temperature with secondary antibody (diluted 1:10000 in PBS-T with 1.5% BSA) that is coupled with horseradish peroxidase (HRP). For detection of His-tags, an α -His-HRP conjugate (Qiagen) was used according to the manufacturer's instructions. Membranes were again washed three times for 15 min with PBS-T. Visualization was performed with Enhanced Chemiluminescence (ECL).

3.4.6 Metabolic labeling with [³H]palmitate

Strains with Bet3 encoding plasmids were grown in WMVIII supplemented with histidine except the AH22*ura3* strain, which was grown in YPD. 25 ml cultures were inoculated at OD₆₀₀ 0.5 and grown to a density of 2.5. 500 μ Ci [³H]palmitate (40-60 Ci mmol⁻¹), 1 μ g ml⁻¹ cerulenin (Sigma), and 1 mM CuSO₄ were added to the cells, and cultures were incubated over night. Cells were harvested and lysed with glass beads in 50 mM Tris, pH 7.5, 5 mM EDTA, 0.5% SDS and 1 mM PMSF. Lysates were cleared by centrifugation (10 min, 13000x g) and diluted 5-fold with 20 mM Tris, pH 8, 150 mM NaCl, 1 mM NaCl and a pull-down was performed using StrepTactin MacroPrep resin (IBA, Germany) for 1 hour at 4 °C. Samples were washed with the same buffer and boiled in SDS loading buffer containing

2.5 mM D-desthiobiotin. Proteins were separated by SDS-PAGE, the gel was fixated with 10% acetic acid and soaked with Amplify (Pharmacia), dried, and subjected to fluorography.

3.4.7 Membrane preparations and extractions

Yeast microsomes were prepared as described [91] from a crude protein extract obtained by lysis with glass beads in 1 ml 50 mM Hepes, pH 7.5, 5 mM EDTA and 1 mM PMSF. HEK293 cells were trypsinized and lysed in 500 μ l 20 mM Hepes, pH 7.4, 100 mM KCl and 2 mM EDTA by sonication for 30 sec on ice. Samples were first centrifuged at 1000x g for 5 min and the supernatant was subjected to ultracentrifugation at 120,000x g for 30 min. The supernatant containing cytosol was removed from the pellet (microsomal fraction).

For extractions membranes were treated with buffer (50 mM Tris, pH 7.5, 5 mM EDTA, 1 mM PMSF), 0.5 M NaCl, 2 M urea, 0.1 M Na₂CO₃, 1 % Triton X-100, or 1 % SDS and incubated on ice for 30 min. Samples were separated into pellet and supernatant (30 min, 14,000x g) and supernatants were subjected to acetone precipitation. Fractions were analyzed by SDS-PAGE and immunoblotting.

3.4.8 Tetrad analysis

Bet3 constructs were transformed in a yeast *bet3* deletion strain (Y25984). A 2 ml YPD culture was inoculated with a single colony and grown for 3 h at 30 °C. Cells were harvested, washed three times with water, resuspended in sporulation media and shaken 2-3 days at 30 °C. Individual spores were dissected on selective plates with a dissecting microscope by Dr. E. Jarosch

3.4.9 Palmitoylation assay and depalmitoylation of Bet3

A standard palmitoylation reaction contained purified Bet3 (5-10 μ l, 8 μ g, 3.2 μ M), 5 μ l [³H]-Pal-CoA (5 pMol, 50 nM), 1mM DTT in a final volume of 100 μ l Tris/NaCl buffer (20 mM Tris/HCl, pH 8.5, 120 mM NaCl) and was incubated for 30 min at 30 °C. Samples were precipitated with 1 ml chloroform/methanol (1:1) and pelleted 15 min at 14,000x g. Pellets were washed with 1 ml methanol, air-dried and subjected to SDS-PAGE and fluorography. Palmitoylation assays were carried out by Dr. M. Veit.

To gently deacylate Bet3, purified protein was incubated with 1 M hydroxylamine (pH 7) for 1 h at 4 °C.